0026-895X/98/010078-08$3.00/0

MOLECULAR PHARMACOLOGY, **53:**78–85 (1998).

Etoposide Targets Topoisomerase IIα and IIβ in Leukemic Cells: Isoform-Specific Cleavable Complexes Visualized and Quantified *In Situ* by a Novel Immunofluorescence Technique

E. WILLMORE, A. J. FRANK, K. PADGET, M. J. TILBY, and C. A. AUSTIN

Department of Biochemistry and Genetics (E.W., K.P., C.A.A.), LRF Unit (A.J.F.), and Cancer Research Unit (M.J.T.), The Medical School, The University of Newcastle-upon-Tyne, Newcastle-upon-Tyne NE2 4HH, United Kingdom

Received December 26, 1997; Accepted April 8, 1998

This paper is available online at http://www.molpharm.org

ABSTRACT

We have shown that both DNA topoisomerase (topo) IIα and β are in vivo targets for etoposide using a new assay which directly measures topo IIα and β cleavable complexes in individual cells after treatment with topo II targeting drugs. CCRF-CEM human leukemic cells were exposed to etoposide for 2 hr, then embedded in agarose on microscope slides before cell lysis. DNA from each cell remained trapped in the agarose and covalently bound topo II molecules from drug-stabilized cleavable complexes remained associated with the DNA. The covalently bound topo II was detected *in situ* by immunofluorescence. Isoform-specific covalent complexes were detected with antisera specific for either the α or β isoform of topo II followed by a fluorescein isothiocyanate-conjugated second antibody. DNA was detected using the fluorescent stain Hoechst 33258. A cooled slow scan charged coupled device camera was used to capture images. A dose-dependent increase in green immunofluorescence was observed when using antisera to either the α or β isoforms of topo II, indicating that both isoforms are targets for etoposide. We have called this the TARDIS method, for trapped in agarose DNA immunostaining. Two key advantages of the TARDIS method are that it is isoform-specific and that it requires small numbers of cells, making it suitable for analysis of samples from patients being treated with topo II-targeting drugs. The isoform specificity will enable us to extend our understanding of the mechanism of interaction between topo II-targeting agents and their target, the two human isoforms.

DNA topo II (EC 5.99.1.3), a nuclear enzyme that controls DNA topology, is the target for many anti-cancer drugs. The enzyme exists as two distinct isoforms (termed α and β) that differ in many respects, including cell cycle regulation and nuclear localization (Wang, 1996; Austin and Marsh, 1998). The enzyme modifies DNA structure by making a double strand break, thus creating a "gate" through which another DNA duplex can pass. After strand passage, the break is ligated and the DNA structure is restored (Liu *et al.,* 1980). This process facilitates cellular processes that require modifications in DNA topology, including replication, transcription, and repair. Many topo II-targeting anti-cancer agents are cytotoxic via stabilization of the normally transient "cleavable" complex. In the drug-stabilized cleavable complex, topo II molecules are covalently bound to DNA strand ends at the double strand break, thereby preventing religation of the DNA strands (Osheroff, 1989). These stabilized complexes are thought to be lethal upon DNA replication when the break becomes permanent, leading to mutations, recombination events, and chromosome aberrations (Chen *et al.,* 1996; Suzuki *et al.,* 1997).

Development of resistance to topo II-targeting drugs is a major clinical problem, and cell line studies have revealed that resistance may be dependent on many factors, including mutations in the topo II genes (Patel and Fisher, 1993; Dereuddre *et al.,* 1995) resulting in decreased catalytic activity (Charcosset *et al.,* 1988) or decreased protein levels (Mirski *et al.,* 1993), increased drug efflux by overexpression of the *mdr1* and *MRP* genes (Long *et al.,* 1991; Lorico *et al.,* 1995), and/or alterations in DNA repair rates (Ritke *et al.,* 1994).

One approach to studying topo II drug sensitivity *in vivo* has been the use of a yeast model system, in which yeast carrying a topo II temperature-sensitive mutation can be rescued by plasmid-borne cDNAs encoding human topo IIα or β (Meczes *et al.,* 1997). This system highlighted differences in drug sensitivities between the two isoforms and will be useful for analysis of drug resistance mutations in topo II genes and screening for isoform-specific drugs. Another approach is the *in vitro* cleavage assay, which has been used to analyze the sequence specificity of both

This work was supported by the Leukaemia Research Fund Grants 9526 and 9644 and the Cancer Research Fund Grant SP1621. K. P. was supported by a studentship from the Kay Kendall Leukaemia Research Fund.

ABBREVIATIONS: Topo, topoisomerase; PBS, phosphate-buffered saline; FITC, fluorescein isothiocyanate; TARDIS, trapped in agarose DNA immunostaining.

isoforms in the presence of anti-topo II agents. Using this assay it has been shown that both the α and β isoforms formed cleavable complexes *in vitro* with mAMSA, teniposide and anthracyclines (Cornarotti *et al.,* 1996; Marsh *et al.,* 1996).

The most well documented model is that of mammalian cell lines, and various techniques have been used to estimate cellular topo content and activity in cell lines and clinical samples. These methods include preparation of whole cell or nuclear extracts for immunoblotting and decatenation/relaxation assays (Danks *et al.,* 1988; Drake *et al.,* 1989) and measurement of topo II mRNA and protein levels (Brown *et al.,* 1995; Houlbrook *et al.,* 1995). These data give an indication of topo abundance *in vitro*, but protein levels do not necessarily reflect enzyme activity or ability to interact with the drug *in vivo*. The extent and type of DNA strand breaks after treatment with anti-topo II agents are often measured by alkaline elution (Pommier *et al.,* 1994). This technique has been used to show that etoposide introduces protein-associated strand breaks in a dose-dependent manner, reaching a maximum after 2 hr of treatment (Kalwinsky *et al.,* 1983; Long *et al.,* 1985). Alkaline elution is very sensitive and has proved invaluable in the analysis of strand breaks; however, it does require a relatively large number of cells, and it cannot distinguish between breaks mediated via DNA topo IIα or β.

We report the development of a new *in situ* assay to quantify drug-stabilized cleavable complex formation in individual cells by immunofluorescence with isoform-specific antibodies. The assay was adapted from the method for quantification of melphalan-DNA adducts (Frank *et al.,* 1996). We have focused on the effects of etoposide (VP-16, a widely used epipodophyllotoxin) on human leukemic CCRF-CEM cells. This technique has a number of advantages. It detects DNA topo II covalently linked to DNA in drug-stabilized, cleavable complexes (rather than strand breaks revealed after proteinase K treatment); the use of isoform-specific antisera allows cleavable complexes containing either DNA topo IIα or β to be distinguished; and it requires only small numbers of cells.

Materials and Methods

Cell culture. The CCRF-CEM human leukemic cell line was maintained as a suspension culture at 37° (in a humidified atmosphere of 5% CO_2) in RPMI 1640 medium supplemented with 10% fetal bovine serum and penicillin (50 units/ml)/streptomycin (50 μg/ml) (cell culture reagents from Gibco/BRL, Paisley, UK). The cells were found to be free from *Mycoplasma* sp. contamination.

Drug treatments and irradiation. Etoposide (1 mg/ml stock dissolved in methanol and stored at −20°) was purchased from Sigma (Poole, Dorset, UK). Exponentially growing cells (~4 × 10^5/ml) were exposed to etoposide for 2 hr. They were then washed by centrifugation (1000 × *g*, 5 min) twice and resuspended in PBS (2.7 mM KCl, 13.7 mM NaCl, 1.5 mM KH_2PO_4, 8 mM Na_2HPO_4, pH 7.2, 0°). To study loss of cleavable complexes, drug-treated cells were washed by centrifugation and incubated in fresh medium for various time periods before being finally washed and resuspended in PBS (0°). For irradiation experiments, cells were irradiated in PBS (0°) at 4 Gy/min using a ^{137}Cs source (Gammacell 1000; Nordion Int., Kanata, Ontario, Canada).

Antibodies. Anti-topo II polyclonal antibodies raised in rabbits were used for these experiments. 18511 was raised to recombinant human topo IIα and 18513 to a recombinant human topo IIβ carboxyl-terminal fragment. Western blots demonstrated that 18511 detected the α isoform specifically and 18513 detected the β isoform specifically (data not shown). In these assays, 18511(α) was used at a 1:50 dilution and 18513 (β) at 1:250. The anti-rabbit FITC-conjugated second antibody ($F(ab')_2$ fragment (Sigma, Poole, Dorset, UK) was used at 1:100 dilution. The mouse anti-histone antibody, which detects H1, H2A, H2B, H3, and H4 (Boehringer Mannheim, Germany), was used at a 1:30 dilution, and the anti-mouse FITC conjugate (Sigma, Poole, Dorset, UK) was used at 1:100.

Agarose embedding and staining. The method for precoating microscope slides and embedding cells in agarose was as described previously (Frank *et al.*, 1996). In brief, 50 μl of cell suspension was warmed to 37° and immediately mixed with an equal volume of agarose solution [2% (w/v) in PBS; "SeaPrep" ultra-low gelling; FMC Bioproducts, Rockland, ME], which had been melted and kept at 37°. The mixture was immediately spread evenly across a slide, and the agarose was quickly gelled by placing the slides on a cold surface (0°). The slides were then immersed in lysis buffer for 15 min at 20°. This lysis buffer contained 1% (w/v) sodium dodecyl sulfate, 80 mM phosphate buffer, pH 6.8, 10 mM EDTA, and a protease inhibitor mixture (2 μg/ml pepstatin A, 2 μg/ml leupeptin, 1 mM phenylmethylsulfonyl fluoride, 1 mM benzamidine, and 1 mM dithiothreitol, final concentrations). In the lysis buffer, 1% Sarkosyl may be successfully substituted for 1% sodium dodecyl sulfate. At this stage slides could be stored at −20° in PBS containing 10% glycerol without loss of signal. Slides were next immersed in 1 M NaCl supplemented with the protease inhibitor mixture for 30 min at 20°, and then washed by immersion three times (5 min per wash) in PBS. Slides were exposed to primary antibody (diluted in PBS containing 0.1% (v/v) Tween 20 and 1% (w/v) bovine serum albumin) for 1 hr in a humidified atmosphere, then washed three times in PBS containing 0.1% (v/v) Tween 20 (PBST). Slides were similarly exposed to the FITC-conjugated second antibody (diluted in PBS containing 0.1% (v/v) Tween 20 and 1% (w/v) bovine serum albumin) for 1 hr before two washes in PBST and one final wash (30 min or overnight at 4°) in PBS containing the protease inhibitor mixture. It was found that increasing the length of incubation time for primary and/or secondary antibodies did not increase fluorescence levels (data not shown), indicating saturation of antibody binding within 1 hr. Slides were stained with Hoescht 33258 (10 μM in PBS; Sigma, Poole, Dorset, UK) for 5 min before application of coverslips that were secured with a sealant. We have termed this technique TARDIS.

Quantitative fluorescence microscopy and image analysis. This was described in detail previously (Frank *et al.,* 1996). In brief, an epifluorescence microscope (Olympus BH2-RFCA, 10× objective) was used to separately visualize the blue (hoechst-stained DNA) fluorescence and the green (FITC-stained topo II) immunofluorescence. Images were captured at an accuracy of 16 bits per pixel using a cooled slow-scan charge-coupled device camera (Astrocam, Cambridge, UK). DNA in a particular field of view was focused only under blue fluorescence to minimize photo bleaching of FITC. An image was then captured of blue fluorescence (5-sec exposure) and then a further image of the same field of view was captured of green fluorescence (20-sec exposure) by using specific filter sets. An average of eight pairs of images per drug dose were captured from replicate slides for each antibody (this gave a total of 100–150 cells per dose for each antibody)

Images were analyzed using Imager 2 software (Astrocam Ltd, UK) based on Visilog 4 (Neosis, France) as described previously (Frank *et al.,* 1996). Briefly, background correction procedures were carried out on each image to correct for any stray light and camera background. Additionally, all images were subjected to blue and green shade correction procedures to compensate for variation in intensity of illumination and nonuniformities in light transmission. Corrected images of blue fluorescence were used to define the areas containing the DNA in each cell, through the creation of a separate binary image. A standardized sequence of image processing functions was applied to the images of each field of view to eliminate from the analysis small particles and objects adjoining the edge of the

image and subtract a background intensity value calculated for each image. The blue and green fluorescence intensities of all pixels in each object (i.e., the area occupied by DNA from an individual cell) were integrated. The small proportion of objects that consisted of more than one cell were excluded from analysis. Statistical analysis was carried out using GraphPad Prism software (Cherwell Scientific, Oxford, UK).

Cytotoxicity assay. CCRF-CEM cells were seeded (5×10^4/ml) into 6-well plates. After 48 hr, the cells were exposed to etoposide for 2 hr, then washed in PBS and incubated in fresh medium. After 5 days, cells were counted by trypan blue exclusion, and the results were expressed as described previously (Boulton *et al.,* 1995) as a percentage of growth inhibition compared with controls.

Results

Immunofluorescent staining of cleavable complexes via agarose embedding. CCRF-CEM cells were exposed to a range of concentrations of etoposide for 2 hr. The newly developed assay (illustrated in Fig. 1) was used to detect drug-stabilized topo IIα- and β-cleavable complexes in individual cells from these cultures. Cells (with/without drug treatment) were embedded in agarose on microscope slides and lysed to remove the cell membrane and soluble proteins. Salt extraction removed nuclear proteins including noncovalently bound topo II. Drug-stabilized covalent topo II-DNA complexes remained and were detected by staining replicate slides (from the same culture) using either 18511(α) or 18513(β) antisera followed by an FITC-conjugated second antibody.

Fig. 2 shows four pairs of images typical of those seen after staining with the 18511(α) antibody. Fig. 2, A, C, E, and G show DNA-specific blue Hoechst-staining of cells for all

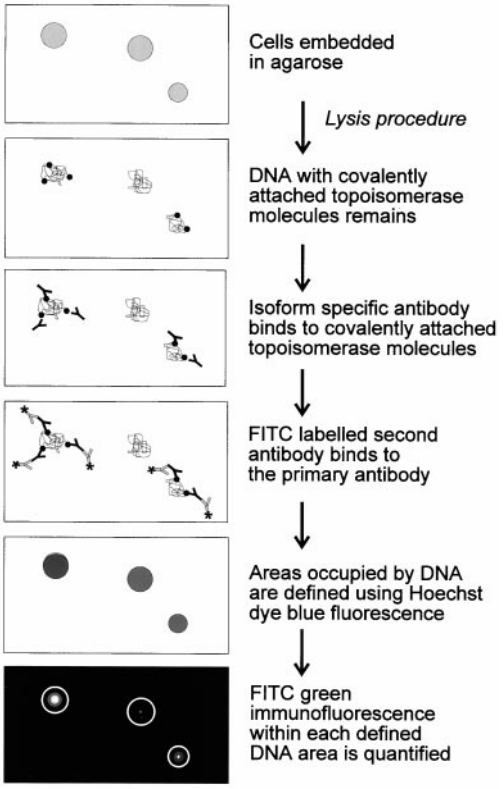

Fig. 1. Schematic diagram of the agarose-embedding method to detect DNA topo II-cleavable complexes.

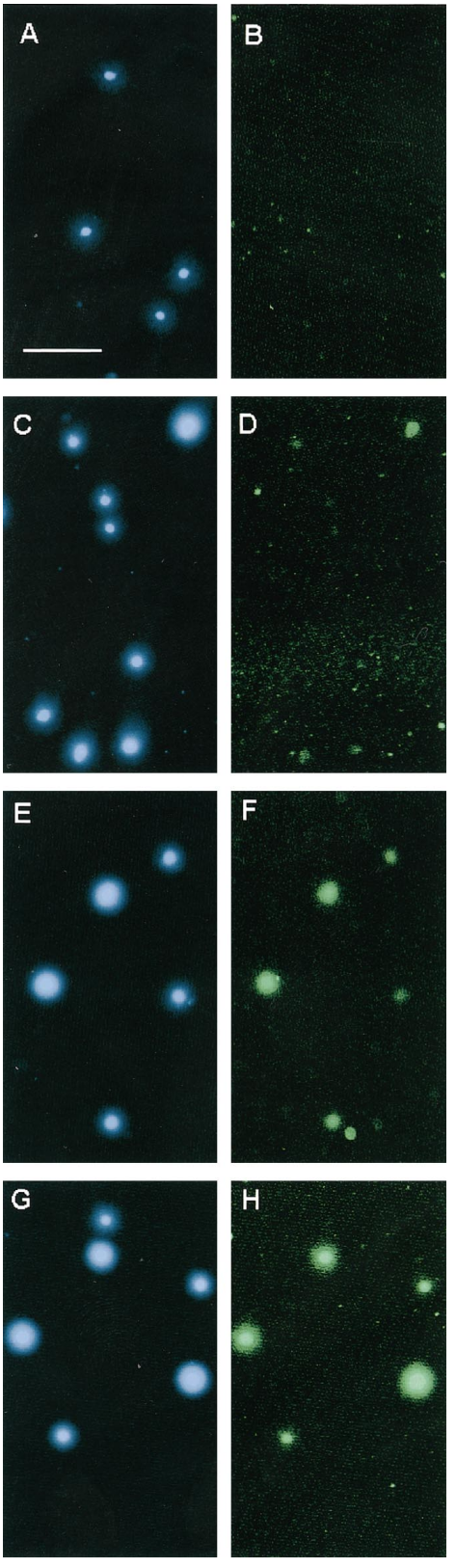

Fig. 2. Fluorescence of etoposide-treated CCRF-CEM cells. Cells were treated with 0 (A, B), 1 (C, D) 10 (E, F), or 100 μM (G, H) etoposide for 2 hr before embedding and staining with 18511(α) Images A, C, E, and G show the Hoechst-stained DNA (*blue*), whereas images B, D, F, and H show the corresponding FITC-stained (*green*) immunofluorescence due to etoposide-stabilized cleavable complexes. (All images were captured under 10× objective and were typical of those seen in replicate experiments). *Bar*, 100 μM.

doses. There was no visible green immunofluorescence associated with DNA in untreated cells (Fig. 2B) or those treated with 0.1 μM etoposide (not shown), but at 1 μM there was detectable immunofluorescence (Fig. 2D). The 10 and 100 μM doses (Fig. 2, F and H) gave very high levels of fluorescence, demonstrating that the staining intensity was dose-dependent. No FITC staining was observed in drug-treated cells when primary antibodies were omitted (data not shown). The intensities of DNA fluorescence and immunofluorescence were heterogeneous, with some cells staining more strongly than others.

Similar images were observed using the 18513(β) antisera, with a dose-dependent increase in immunofluorescence (results not shown). Importantly, we have also tested five other antibodies in this system, but of these only two (α-specific rabbit polyclonal purchased from TopoGEN (Columbus, OH), and β-specific rabbit polyclonal kindly provided by Dr. D. Sullivan, Moffitt Cancer Center, Tampa, FL) gave a strong enough signal to allow preliminary analysis, indicating that not all antibodies are suitable for this assay.

Quantification and analysis of results. Digital images of Hoechst (DNA) fluorescence and FITC immunofluorescence were subjected to correction and analysis procedures to quantify the blue and green fluorescence associated with the DNA from each cell. Detailed results for a typical experiment in which the DNA was stained with 18511(α) are shown in Figs. 3 and 4. Fig. 3, a and b, shows scattergrams in which every cell that was analyzed is depicted as a dot. This representation of results shows not only the wide range of fluorescence values for Hoechst (DNA) staining, but also the existence of two distinct populations of cells at the highest doses (Fig. 3a). FITC immunofluorescence values (Fig. 3b) did not vary considerably for the untreated cells and 0.1 μM dose, but did begin to show a wide spread of values for the 10 and 100 μM doses.

FITC immunofluorescence increased in a dose-dependent manner (Fig. 3d) and for 1 μM and above, the values were significantly higher than in the untreated cells ($p < 0.001$, Mann-Whitney test). There was a 150-fold increase in integrated FITC immunofluorescence comparing untreated cells and those treated with 100 μM etoposide. Hoechst fluorescence also increased with dose, but only by 3-fold, and this increase reached a plateau at 1 μM.

The representative histograms shown in Fig. 4 demonstrate that the distributions of integrated fluorescence intensities for FITC immunofluorescence (and Hoechst fluorescence, data not shown) were mostly non-Gaussian (Kolmogorov-Smirnov test). For this reason, median fluores-

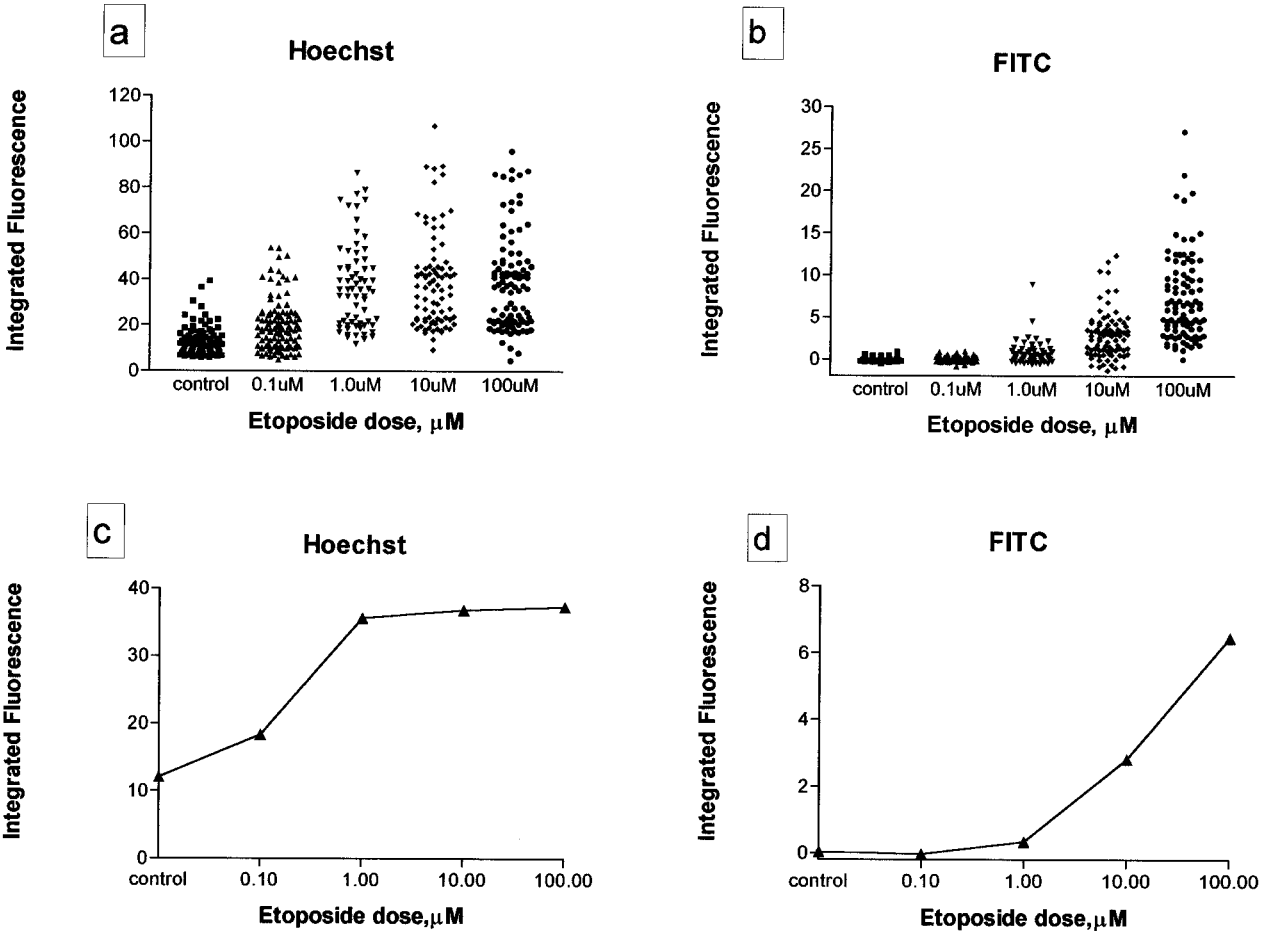

Fig. 3. Dose-dependent nature of fluorescence after etoposide treatment. Cells were treated with 0, 0.1, 1, 10, and 100 μM etoposide for 2 hr, and then slides were prepared. These were stained with 18511(α) and processed and analyzed as described in the text. Scattergrams show fluorescence levels for each individual cell for Hoechst (a) or FITC (b). Plots of median fluorescence values are shown for Hoechst (c) or (d) FITC, with the drug dose shown on a log scale for clarity. Integrated fluorescence values on all *y*-axes have been reduced for simplicity by 10^{-4}. The data were obtained from one experiment typical of five other independent experiments.

cence values were used for individual experiments. Fig. 4a shows that, for untreated cells, although the median level is around zero, there are several cells with negative fluorescence values. This phenomenon was often observed for the untreated cells and lower doses, and reflects the way in which the image analysis procedures were carried out. The integrated green fluorescence value associated with the DNA from each cell was calculated after subtraction of the background fluorescence (calculated as the mean fluorescence intensity of all pixels lying between the DNA objects). Fluorescence is not discernible in the control specimens, and when plotted as a histogram, the immunofluorescence intensities form a distribution centered on zero (reflecting the image correction procedures) and the median was not significantly different to zero ($p = 0.125$). The histograms for the 1 μM dose (Fig. 4b) and 100 μM dose (Fig. 4c) show the dose-dependent increase in immunofluorescence values, producing a shift to the right in the frequency distribution.

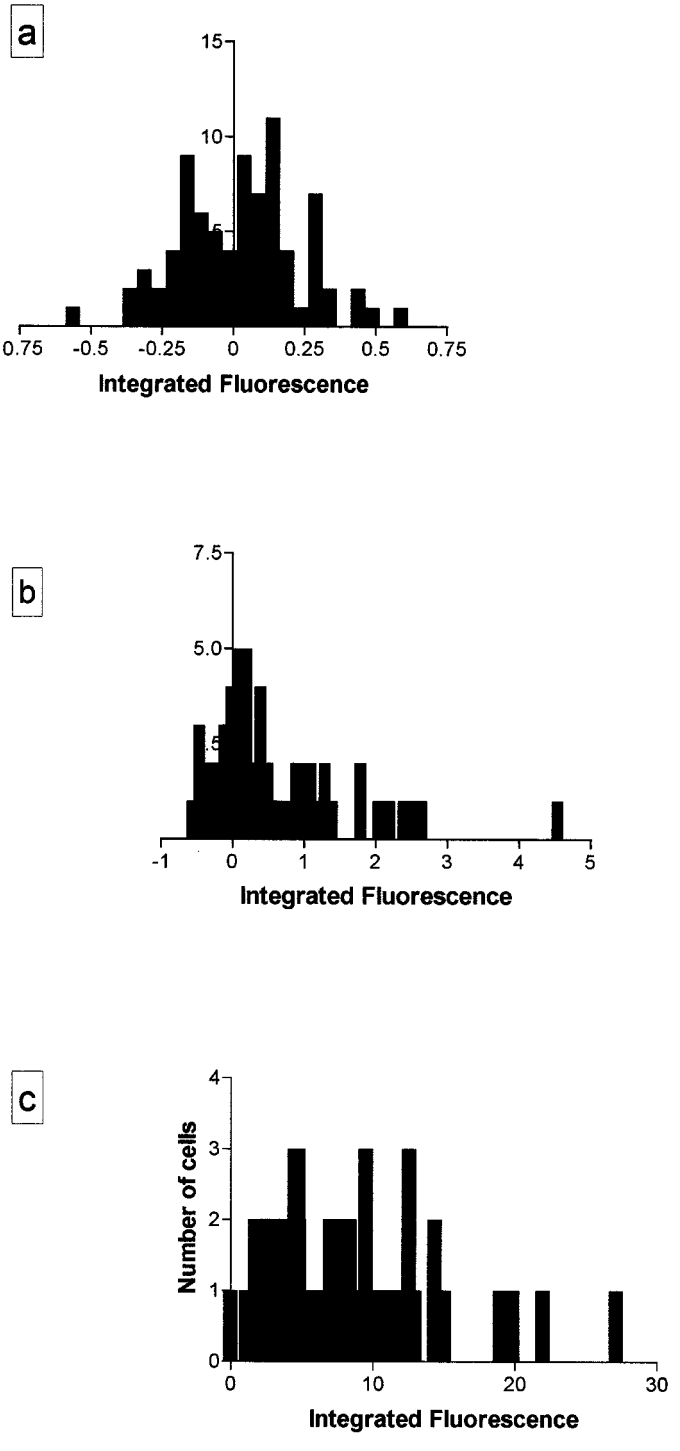

Fig. 4. Histograms show the frequency distribution of immunofluorescence for untreated cells (a) or for cells treated with 1 μM (b) or 100 μM (c) etoposide and stained with 18511(α). The data were obtained from one experiment which was typical of five others.

Fig. 5 summarizes the results of three to six independent experiments for each antibody. Fig. 5, a and c, show that the increase in Hoechst fluorescence is a consistent observation. Fig. 5, b and d, show the dose-dependent increase in FITC immunofluorescence for both 18511(α) and 18513(β) antisera. For the α isoform, the FITC immunofluorescence values for 1, 10, and 100 μM etoposide were highly significant (at the 95% confidence level, $p = 0.0056$, 0.0011, and 0.0002, respectively, t test). For the β isoform, the FITC immunofluorescence values for 10 and 100 μM etoposide were highly significant ($p = 0.0002$ and 0.0001 respectively). These results illustrate that the formation of cleavable complexes after etoposide treatment involves both isoforms of topo II.

Specificity of complex recognition. To confirm that the immunofluorescence detected by this technique was specific for topo II cleavable complexes, the following experiments were performed.

First, Fig. 6 shows the immunofluorescence values for cells after removal of etoposide and incubation in drug-free medium for various times before slide preparation for the α isoform (a) and the β isoform (b). Fig. 6a shows that, after 30 min, the integrated fluorescence level for the 100 μM dose was 2-fold lower than that seen in cells embedded immediately after drug treatment. After 60 min, the levels were reduced further, and after 120 min there was little or no immunofluorescence at any dose of etoposide, consistent with virtually all of the cleavable complexes having disassociated. Interestingly, Fig. 6b shows that the kinetics of reversal of drug-stabilized complexes may be different for the β isoform. After only 30 min, the integrated fluorescence level for the 100 μM dose was already reduced to that seen in untreated cells, indicative of complete reversal of etoposide-stabilized β cleavable complexes within this time period. Indeed, after only 15 min of incubation in drug-free medium, the integrated fluorescence level for the 100 μM dose was 2-fold less than that seen in cells embedded immediately after drug treatment.

Second, cells were exposed to ionizing radiation (10 and 50 Gy) and immediately embedded in agarose, lysed, and stained to test the specificity of 18511(α) or 18513(β) antisera for a different type of DNA damage. Ionizing irradiation damage results in ss and ds breaks (as well as cross-links/DNA-protein cross-links as minor products). The results showed that the integrated immunofluorescence levels for both 10 and 50 Gy were in the same range as the levels from nonirradiated cells (data not shown). Taken together, these results strongly suggest that the immunofluorescence detected by these antibodies using this method is specific for topo-II stabilized cleavable complexes.

Third, cells were treated with 10 μM etoposide for 2 hr, immediately embedded in agarose, and lysed. They were stained with an anti-histone antibody and FITC-conjugated second antibody. When images were captured (using the

same exposure conditions as for anti-topo II immunofluorescence), analysis showed that there was no detectable immunofluorescence regardless of whether slides had been treated with 1 M NaCl (data not shown).

Cytotoxicity. Fig. 7 shows the cytotoxic effect of etoposide on CCRF-CEM cells after a 2-hr exposure. The IC_{50} value for etoposide is ~1 μM, and there were no surviving cells at either 10 or 100 μM.

Discussion

We have shown for the first time that both isoforms of human DNA topo II are targeted by etoposide *in vivo*. This report describes a novel "TARDIS" method with which etoposide-induced topo IIα- and β-cleavable complex formation in individual cells can be visualized and quantified. Using this method, we have shown that both isoforms form cleavable complexes *in vivo* after etoposide treatment in a dose dependent manner. This confirms the previously obtained *in vitro* data (Cornarotti *et al.,* 1996; Marsh *et al.,* 1996) and data from a yeast model system (Meczes *et al.,* 1997), which indicated that both isoforms were potential targets for etoposide.

The results showed that the increase in immunofluorescence intensity was dependent on etoposide concentration (Figs. 3 and 4), becoming highly significant at 10 and 100 μM doses ($p < 0.0001$, Mann-Whitney test) The actual values for immunofluorescence (at 100 μM etoposide) were approximately 5-fold higher for the 18511(α) antibody than they were for the 18513(β) antibody (Fig. 5, b and d). This initially suggests that the α isoform may be a better target for etoposide in these cells, possibly because it is more sensitive to stabilized complex formation. However, it cannot be assumed that the higher values for the α antibody directly reflect actual enzyme quantities, because the efficacy of one antibody compared with the other is not known.

Several observations confirmed that the immunofluorescence measured in this assay was specific for topo II-cleavable complexes. First, it is well documented that the cleavable complexes are reversible. After removal of the drug, the equilibrium between topo II trapped in cleavable complexes and unbound topo II carrying out its normal cleavage/religation reaction shifts back toward unbound topo II (Hsiang and Liu, 1989). This manifests itself in the loss of drug-induced DNA strand breaks (Caldecott *et al.,* 1993) and in this case, in a time-dependent decrease in immunofluorescence consistent with the disassociation of cleavable complexes.

Second, 18511(α) and 18513(β) antisera bound specifically to topo II proteins stabilized in the cleavable complex and not

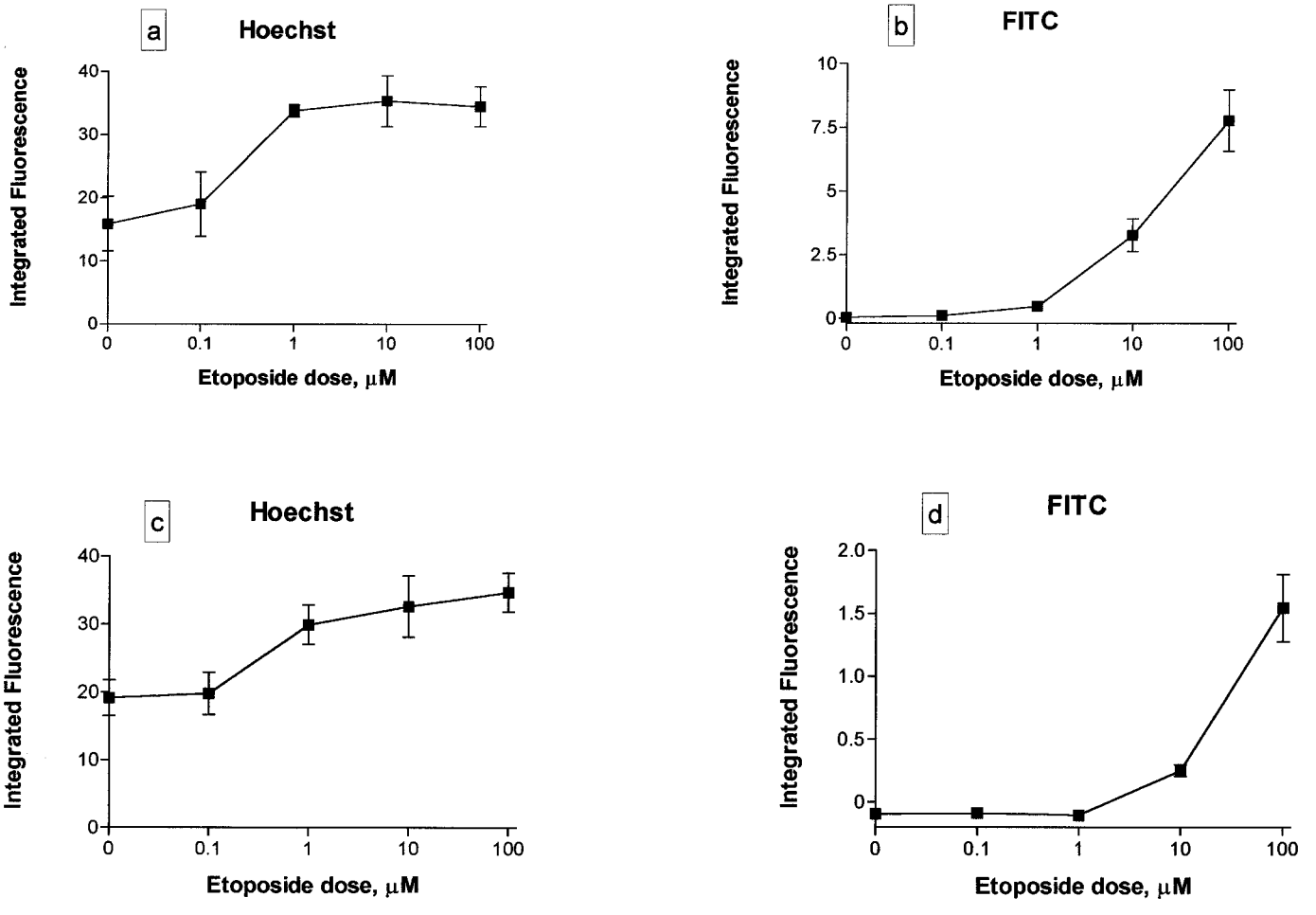

Fig. 5. Summary of data of three to six independent experiments. Cells were treated exactly as described in Fig. 3, but here data are presented for both antibodies. Plots show means ± standard error bars calculated from median fluorescence values obtained from independent experiments. a and c, Hoechst fluorescence for cells treated with 18511(α) or with 18513(β) respectively; b and d, FITC immunofluorescence values for 18511(α) or 18513(β), respectively.

to other DNA strand breaks, as illustrated by the use of irradiated cells. Third, the staining of drug-treated cells with an anti-histone antibody did not result in any detectable levels of immunofluorescence, demonstrating that the lysis procedure removes histones and probably other nuclear proteins, leaving only stabilized topo II-cleavable complexes.

In addition to the significant increase in immunofluorescence after etoposide treatment, there was also a small increase in the Hoechst fluorescence (Fig. 5, a and c). However, this increase reached a plateau by 1 μM and was not dose-dependent at higher etoposide concentrations. Hoechst is a minor groove binding dye that binds most strongly to double-stranded DNA with a preference for AT-rich sequences (Vega *et al.,* 1996 and references therein). The increase in Hoechst fluorescence was presumably caused by a change in DNA conformation resulting from inhibition of topo II, because the 2-hr etoposide exposure period was too short to permit significant accumulation of G_2 cells and concomitant increase in DNA content.

The IC_{50} value for growth inhibition by etoposide was found to be 1 μM (Fig. 7). The results from Figs. 3 and 4 demonstrated that cleavable complexes became detectable at 1 μM, suggesting that relatively low levels of etoposide-induced complexes trigger events leading to cell death. This implies that the cleavable complex is a highly cytotoxic lesion, but it is likely that events downstream of complex formation [e.g., inhibition of replicon initiation (Kaufmann *et al*., 1991) DNA strand breaks, sister chromatid exchanges (Chaterjee *et al*., 1990), and other chromosome aberrations (Chen *et al*., 1996)] are ultimately responsible for cell death. The mechanism responsible for topo II-cleavable complex formation by etoposide is now well defined. Etoposide stimulates the ability of topo II to break double-stranded DNA after strand passage of the duplex (Robinson and Osheroff, 1991), and the stabilized complexes then result in a reversible inhibition of religation of the DNA (Sehested and Jensen, 1996). Interestingly, it was recently postulated that it is the interaction between topo II and etoposide (rather than between etoposide and DNA) that directs the formation of cleavable complexes at specific sequences, resulting in inhibition of religation (Burden *et al.,* 1996). In addition, etoposide-induced DNA damage has been shown to trigger apoptosis in many cell lines (e.g., Kamesaki *et al.,* 1993), and the role of p53 in determining cell death is particularly important in cancer cells (Chresta *et al.*, 1996; Skladanowski and Larsen, 1997).

In another study, in which cells treated with VM-26 (another cleavable complex-forming epipodophyllotoxin), topo II-cleavable complexes were immunoprecipitated with isoform-specific antibodies. The results obtained demonstrated that topo IIα-cleavable complexes were associated with the replication fork (i.e., nascent DNA), whereas topo IIβ complexes were found in bulk (mature) DNA (Qiu *et al.,* 1996). These results highlight the requirement to differentiate between isoforms and their known cell-cycle dependence when designing drug regimens.

One of the most important currently used assays for detection of etoposide-induced DNA damage is alkaline elution, a technique that has yielded much information about double-, single-, and protein-linked strand break levels and their repair (Long *et al.,* 1985; Caldecott *et al.,* 1990). However, this process requires radiolabeling of cells followed by elution of DNA from filters; it does not distinguish between isoforms and is unsuitable for small (e.g., patient) cell samples. Methods to measure topo II catalytic activity in patient samples (e.g., Cattan *et al.,* 1996) are available, but again, these do not identify isoform-specific differences. The novel immunological technique described here can detect isoform-specific

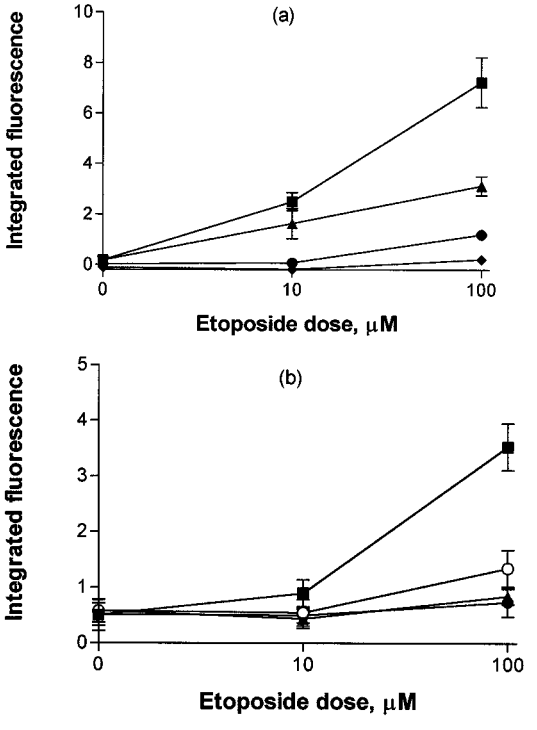

Fig. 6. Disassociation of topo II-cleavable complexes with time. a, Cells were treated with etoposide (0, 10, and 100 μM) for 2 hr, then slides were prepared immediately (■) or after drug was washed out and cells incubated in fresh medium for 30 (▲), 60 (●), or 120 (♦) min. Slides were stained with 18511(α) and processed as described in the text. b, Cells were similarly treated with etoposide, and slides were prepared immediately (■) or after incubation in drug-free medium for 15 (○), 30 (▲), or 60 (●) min. Plot shows mean and mean ± standard error bars for immunofluorescence values obtained from four (a) or three (b) independent experiments.

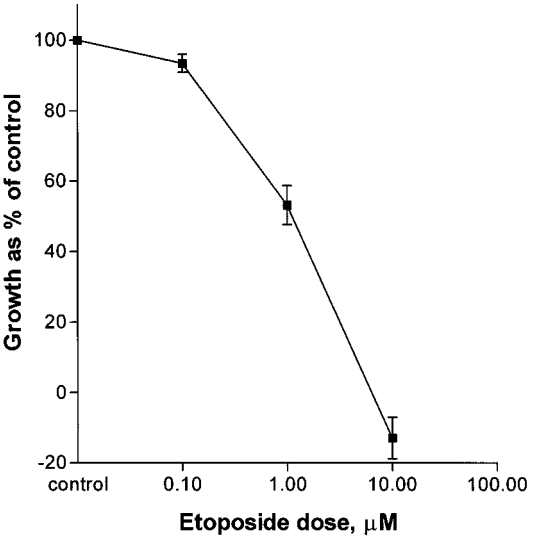

Fig. 7. CCRF-CEM cells were treated with 0, 0.1, 1, 10, or 100 μM etoposide for 2 hr. After exposure, the drug was washed off, and cells were incubated in fresh medium for 5 days. Results are expressed as described in the text. Plot shows the means and mean ± standard error bars obtained from four independent experiments.

antibody interactions, which directly reflect cleavable complex formation in individual cells. In combination with data generated using assays that reveal information about events downstream of cleavable complex formation, this assay should assist in providing a wider understanding of the mechanism of action of topo II-targeting drugs. Work in progress with other topo II-targeting agents that form cleavable complexes indicates that it is possible to detect cleavable complex formation in CCRF-CEM cells after treatment with these drugs.

The advantage of being able to study intercell heterogeneity for both α and β isoforms in cell lines and clinical samples should facilitate better chemotherapeutic regimens. In the light of the data shown in Fig. 6, it will be interesting to measure the disappearance of cleavable complexes in pairs of sensitive and resistant cells. It has been shown that some etoposide-resistant cells have a defect in cleavable complex stability, allowing them to repair more quickly (Ritke *et al.,* 1994). It is possible that the level of complex formation/rate of disappearance (which may differ between isoforms) in resistant cells would provide a useful prognostic marker that could be assessed using this immunofluorescence assay. In patients, "low dose" (<1500 mg/m^2) etoposide results in a serum concentration of ~2 μM, whereas "high dose" (>4000 mg/m^2) results in a concentration of ~10 μM (Joel, 1996). Because these doses are at the lower end of the range used for our *in vivo* experiments, it may be possible to use this technique to investigate the resistance status of patients receiving this type of treatment. For example, a patient sample containing a significant subpopulation of resistant cells would give a very low integrated fluorescence signal that might predict a poor response to therapy. Indeed, work is currently in progress to quantify topo IIα- and β-cleavable complex formation in samples from leukemia patients undergoing etoposide therapy.

References

Austin CA and Marsh KL (1998) Eukaryotic DNA topoisomerase IIβ. *Bioessays* **20:**215–226.

Boulton S, Pemberton LC, Porteous JK, Curtin NJ, Griffin RJ, Golding BT, and Durcacz BW (1995) Potentiation of temozolamide-induced cytotoxicity: A comparative study of the biological effects of poly(ADP-ribose) polymerase inhibitors. *Br J Cancer* **72:**849–856.

Brown GA, McPherson JP, Gu L, Hedley DW, Toso R, Deuchars KL, Freedman MH, and Goldenberg GJ (1995) Relationship of DNA topoisomerase IIα and β expression to cytotoxicity of antineoplastic agents in human acute lymphoblastic leukemia cell lines. *Cancer Res* **55:**78–82.

Burden AD, Kingma PS, Froelich-Ammon SJ, Bjornsti M, Patchan MW, Thompson RB, and Osheroff N (1996) Topoisomerase II-etoposide interactions direct the formation of drug-induced enzyme-DNA cleavage complexes. *J Biol Chem* **271:** 29238–29244.

Caldecott K, Banks G, and Jeggo P (1990) DNA double-strand break repair pathways and cellular tolerance to inhibitors of topoisomerase II. *Cancer Res* **50:**5778–5783.

Caldecott K, Banks G, and Jeggo P (1993) The induction and reversal of topoisomerase II cleavable complexes formed by nuclear extract from the CHO DNA repair mutant, *xrs*1. *Mutat Res* **293:**259–267.

Cattan AR, Levett D, Douglas EA, Middleton PG, and Taylor PRA (1996) Method for quantifying expression of functionally active topoisomerase II in patients with leukaemia. *J Clin Pathol* **49:**848–852.

Charcosset J, Saucier J, and Jacquemin-Sablon A (1988) Reduced DNA topoisomerase II activity and drug-stimulated DNA cleavage in 9-hydroxyellipticine resistant cells. *Biochem Pharmacol* **37:**2145–2149.

Chaterjee S, Trivedi D, Petzold J, and Berger NA (1990) Mechanism of epipodophyllotoxin- induced cell death in poly(adenosine-diphosphate-ribose) synthesis-deficient V79 Chinese hamster cell lines. *Cancer Res* **50:**2713–2718.

Chen C, Fuscoe JC, Liu Q, and Relling MV (1996) Etoposide causes illegitimate V (D) J recombination in human lymphoblastoid leukemic cells. *Blood* **88:**2210–2218.

Chresta CM, Masters JRW, and Hickman JA (1996) Hypersensitivity of human testicular tumors to etoposide-induced apoptosis is associated with functional p53 and a high Bax:Bcl-2 ratio. *Cancer Res* **56:**1834–1841.

Cornarotti M, Tinelli S, Willmore E, Zunino F, Fisher LM, Austin CA, and Capranico G (1996) Drug sensitivity and sequence specificity of human recombinant DNA topoisomerases IIα (p170) and IIβ (p180). *Mol Pharmacol* **50:**1463–1471.

Danks MK, Schmidt CA, Cirtain MC, Suttle DP, and Beck WT (1988) Altered catalytic activity of and DNA cleavage by DNA topoisomerase II from human leukemic cells selected for resistance to VM-26. *Biochemistry* **27:**8861–8869.

Dereuddre S, Frey S, Delaporte C, and Jacquemin-Sablon A (1995) Cloning and characterisation of full-length cDNAs coding for the DNA topoisomerase IIβ from Chinese hamster lung cells sensitive and resistant to 9-OH-ellipticine. *Biochim Biophys Acta* **1264:**178–182.

Drake FH, Hofmann GA, Bartus HF, Mattern MA, Crooke ST, and Mirabelli CK (1989) Biochemical and pharmacological properties of p170 and p180 forms of topoisomerase II. *Biochemistry* **28:**8154–8160.

Frank AJ, Proctor SJ, and Tilby MJ (1996) Detection and quantification of melphalan-DNA adducts at the single cell level in hematopoietic tumor cells. *Blood* **88:**977–984.

Houlbrook S, Addison CM, Davies SL, Carmichael J (1995) Stratford IJ, Harris AL, and Hickson ID. Relationship between expression of topoisomerase II isoforms and intrinsic sensitivity to topoisomerase II inhibitors in breast cancer cell lines. *Br J Cancer* **72:**1454–1461.

Hsiang Y and Liu LF (1989) Evidence for the reversibility of cellular DNA lesion induced by mammalian topoisomerase II poisons. *J Biol Chem* **264:**9713–9715.

Joel S (1996) The clinical pharmacology of etoposide: An update. *Cancer Treat Rev* **22:**179–221.

Kalwinsky DK, Look AT, Ducore J, and Fridlans A. (1983) Effects of the epipodophyllotoxin VP-16–213 on cell cycle traverse, DNA synthesis, and DNA strand size in cultures of human leukemic lymphoblasts. *Cancer Res* **43:**1592–1597.

Kamesaki S, Kamesaki H, Jorgenson TJ, Tanizawa A, Pommier Y, and Cossman J (1993) bcl-2 protein inhibits etoposide-induced apoptosis through its effects on events subsequent to topoisomerase II-induced DNA strand breaks and their repair. *Cancer Res* **53:**4251–4256.

Kaufmann WK, Boyer JC, Estabrooks LL, and Wilson SJ (1991) Inhibition of replicon initiation in human cells following stabilisation of topoisomerase-DNA cleavable complexes. *Mol Cell Biol* **11:**3711–3718.

Liu LF, Liu CC, and Alberts BM (1980) Type II DNA topoisomerases: enzymes that can unknot a topologically knotted DNA molecule via a reversible double strand break. Cell **19:**697–707.

Long BH, Musiai ST, and Brattain MG (1985) Single- and double-strand DNA breakage and repair in human lung adenocarcinoma cells exposed to etoposide and teniposide. *Cancer Res* **45:**3106–3112.

Long BH, Wang L, Lorico A, Wang RCC, Brattain MG, and Casazza A (1991) Mechanisms of resistance to etoposide and teniposide in acquired resistant human colon and lung carcinoma cell lines. *Cancer Res* **51:**5275–5284.

Lorico A, Rappa G, Srimatkcandada S, Catapano CV, Fernandes DJ, Germino JF, and Sartorelli AC (1995) Increased rate of adenosine triphosphate-dependent etoposide (VP-16) efflux in a murine leukemia cell line overexpressing the multidrug resistance-associated protein (MRP) gene. *Cancer Res* **55:**4352–4360.

Marsh KL, Willmore E, Tinelli S, Cornarotti M, Meczes E (1996) Capranico G, Fisher LM, and Austin CA. Amsacrine-promoted DNA cleavage site determinants for the two human DNA topoisomerase II isoforms α and β. *Biochem Pharmacol* **52:**1675–1685.

Meczes EL, Marsh KL, Fisher LM, Rogers MP, and Austin CA (1997) Complementation of temperature-sensitive topoisomerase II mutations in *Saccharomyces cerevisiae* by a human TOP2β construct allows the study of topoisomerase IIβ inhibitors in yeast. *Cancer Chemother Pharmacol* **39:**367–375.

Mirski SEL, Evans CD, Almquist KC, Slovak ML, and Cole S (1993) Altered topoisomerase IIα in a drug-resistant small cell lung cancer cell line selected in VP-16. *Cancer Res* **53:**4866–4873.

Osheroff N (1989) Effect of antineoplastic agents on the DNA cleavage/religation reaction of eukaryotic topoisomerase II: Inhibition of religation by etoposide. *Biochemistry* **28:**6157–6160.

Patel S, and Fisher LM (1993) Novel selection and genetic characterisation of an etoposide-resistant human leukaemic CCRF-CEM cell line. *Br J Cancer* **67:**456–463.

Pommier Y, Leteurtre F, Fesen MR, Fujimori A, Bertrand R, Solary E, Kohlhagen G, and Kohn KW (1994) Cellular determinants of sensitivity and resistance to DNA topoisomerase inhibitors. *Cancer Invest* **12:**530–542.

Qiu J, Catapano V, Fernandes DJ (1996) Formation of topoisomerase IIα complexes with nascent DNA is related to VM-26 induced cytotoxicity. *Biochemistry* **35:** 16354–16360.

Ritke MK, Roberts D, Allan JR, Bergoltz VV, and Yalowich JC (1994) Altered stability of etoposide-induced topoisomerase II-DNA complexes in resistant human leukaemia K562 cells. *Br J Cancer* **69:**687–697.

Robinson MJ and Osheroff N (1991) Effects of antineoplastic drugs on the post-strand passage DNA cleavage/religation equilibrium of topoisomerase II. *Biochemistry* **30:**1807–1813.

Sehested M and Jensen PB (1996) Mapping of DNA topoisomerase II poisons (etoposide, Clerocidin) and catalytic inhibitors (aclarubicin, ICRF-187) to four distinct steps in the topoisomerase II catalytic cycle. *Biochem Pharmacol* **51:**879–886.

Skladanowski A and Larsen AK (1997) Expression of wild-type p53 increases etoposide cytotoxicity in M1 myeloid leukemia cells by facilitated G_2 to M transition: implications for gene therapy. *Cancer Res* **57:**818–823.

Suzuki H, Tarumoto Y, and Ohsawa M (1997) Topoisomerase II inhibitors fail to induce chromosome-type aberrations in etoposide-resistant cells: evidence for essential contribution of the cleavable complex formation to the induction of chromosome-type aberrations. *Mutagenesis* **12:**29–33.

Vega MC, Coll M, and Aleman C (1996) Intrinsic conformational preferences of the Hoechst dye family and their influence on DNA binding. *Eur J. Biochem* **239:**376–383.

Wang JC (1996) DNA Topoisomerases. *Ann Rev Biochem* **65:**635–692.

Send reprint requests to: Dr. C. A. Austin, Department of Biochemistry and Genetics, The Medical School, Newcastle-upon-Tyne, NE2 4HH, UK. E-mail: caroline.austin@ncl.ac.uk